SLAC-PUB-1641
August 1975
(T/E)

STUDY OF $K^-p \to \bar{K}^*(890)n$ AT 13 GeV *

G. W. Brandenburg†, R. K. Carnegie††, R. J. Cashmore†††, M. Davier‡, W. M. Dunwoodie, T. A. Lasinski, D.W. G.S. Leith, J.A.J. Matthews‡‡, P. Walden‡‡‡, and S. H. Williams

Stanford Linear Accelerator Center
Stanford University, Stanford, California 94305

ABSTRACT

The results of a wire chamber spectrometer experiment studying $\bar{K}^*(890)$ production in the reaction $K^-p \to K^-\pi^+n$ at 13 GeV are presented. Strong forward structure is observed for $|t| < m_\pi^2$ in the s-channel density matrix elements and differential cross section. These features are similar to those observed in $\pi^-p \to \rho^0 n$ data and are characteristic of π exchange. In contrast in the intermediate, $|t| \sim 0.2$ GeV^2, and large momentum transfer regions $\bar{K}^*(890)$ production is dominated by the natural parity ρ-A_2 exchange contribution.

(Submitted for publication)

*Work supported by the U.S. Energy Research and Development Administration.

Present address:
†Department of Physics, MIT, Cambridge, Massachusetts.
††Department of Physics, Carleton University, Ottawa, Ontario, Canada.
†††Department of Physics, Oxford University, Keble Rd., Oxford, England.
‡ Laboratoire de l'Accelerateur Linéaire, Orsay, France.
‡‡Department of Physics, Michigan State University, East Lansing, Michigan.
‡‡‡TRIUMF, University of British Columbia, Vancouver, B. C., Canada.

In this letter we present new results on $\bar{K}^*(890)$ production [1,2] in the reaction $K^- p \to K^- \pi^+ n$ at 13 GeV from a wire spark chamber spectrometer experiment performed at SLAC. In the small momentum transfer region, the data show the characteristic features of the dominant π exchange very clearly: in particular, the pronounced forward turnover of the differential cross section for $|t| < m_\pi^2$ and the striking small t variation of the s-channel density matrix elements. These π exchange features are quite similar to the structure observed in the forward direction in high statistics data on $\pi^- p \to \rho^0 n$ [3,4]. However, in the $\bar{K}^*$ data there exist significant differences which reflect the presence of the additional exchange contributions allowed in the K^--induced reaction. The data sample comprises 14,200 events in the $\bar{K}^*(890)$ region defined as $0.87 < M(K^-\pi^+) < 0.92$ GeV, and extends to a momentum transfer $|t| \sim 1.2$ GeV^2. For $|t| > 0.20$ GeV^2, we find that $\bar{K}^*$ production is dominated by natural parity exchange.

The experiment was performed in an RF separated 13 GeV K beam at SLAC. Fig. 1 shows a plan view of the apparatus [5]. Scintillation counter hodoscopes, two threshold Cerenkov counters, and 1 mm wire spacing proportional chambers were used to measure the mass, momentum, and trajectory of each beam particle incident on the 1 meter long hydrogen target. Beam resolution is ±0.3% in momentum and ±0.5 mrad in angle. The $(K^-\pi^+)$ system was detected in a forward spectrometer which included three scintillation counter hodoscopes and nine magnetostrictive readout wire spark chambers, four upstream and five downstream of an 18 kg m dipole magnet. The dipole aperture was 0.6 m by 1.8 m. Each chamber had small polyurethane plugs installed through which the beam passed. The spectrometer measures the $(K^-\pi^+)$ production angle to better than 1 mrad and the effective mass resolution is ±5 MeV at the $\bar{K}^*(890)$.

The trigger for the experiment required that 2 or more charged particles pass through the spectrometer after originating from a K^- interaction in the hydrogen target. In addition, the magnet was lined with scintillation counters to reject events in which a secondary particle strikes a pole piece. The large aperture Cerenkov counter contained eight optically distinct elements and provided K, π identification of the secondary particles.

Events from the reaction $K^-p \rightarrow K^-\pi^+n$ are selected by requiring that the missing mass of the recoil system fall in the neutron region, 0.70 - 1.05 GeV [6]. In addition, events are rejected if the $\pi^+\pi^-$ hypothesis for the secondary particles corresponds to a K^0 mass or if the K^+K^- hypothesis yields a ϕ meson mass. After these selection criteria are imposed, there still remains a small background (5-10%) from $K^-p \rightarrow K^-\pi^+\Delta^0$ events which fall in the neutron missing mass cut due to the experimental missing mass resolution. This experiment also included a high statistics measurement of the reaction $K^+p \rightarrow K^+\pi^-\Delta^{++}$. The correction of the $K^-\pi^+n$ events for the $K^-\pi^+\Delta^0$ background is made by directly subtracting the properly normalized observed $K^+\pi^-\Delta^{++}$ events which would satisfy the neutron selection criteria from the observed $K^-\pi^+$ angular distribution for each $K\pi$ mass and t bin independently.

The spherical harmonic moments, $\langle Y_{\ell m}\rangle$, of the $K^-\pi^+$ system have been measured as a function of momentum transfer for the $K\pi$ mass interval $0.87 < m(K^-\pi^+) < 0.92$ GeV. The moments are obtained by comparing the experimental $K^-\pi^+$ angular distribution to an acceptance corrected sum of spherical harmonics using a maximum likelihood fitting procedure. The spectrometer acceptance is determined using a Monte Carlo program which incorporates measured apparatus efficiency factors, the effects of secondary K decay, nuclear absorption, and resolution, and subjects the Monte Carlo events to the

identical geometric and kinematic criteria that the experimental data must satisfy. The fits to the $K^-p \to K^-\pi^+n$ data in the $\bar{K}^*(890)$ region have been restricted to ℓ, $m \leq 2$, corresponding to only s and p waves being present, since separate fits with ℓ, $m \leq 4$ yielded no evidence for the presence of d-wave in this $K\pi$ mass region. The results, re-expressed as elements of the spin density matrix, $\rho^{\ell\ell'}_{mm'}$, are presented in Fig. 2 for the s-channel analysis. All of the s-channel moments exhibit a strong variation with momentum transfer.

The $K^-p \to K^-\pi^+n$ differential cross section, $d\sigma/dt$, for $0.87 < m(K^-\pi^+) < 0.92$ GeV is obtained concurrently with the moments and is shown in Fig. 3 for $t < 0.6$ GeV^2. The estimated systematic error in absolute normalization is ±10%. The differential cross section has a maximum for $|t| \sim m_\pi^2$ and exhibits a clear forward turnover indicating the dominance of pion exchange in the small momentum transfer region. There is a distinct break in the slope of the differential cross section near $t \sim 0.15$ GeV^2.

The particular linear combinations of the density matrix elements,

$$\sigma_0 = (\rho^{11}_{00} + \rho^{00}_{00}/3)d\sigma/dt$$

and

$$\sigma_\pm = (\rho^{11}_{11} \pm \rho^{11}_{1-1} + \rho^{00}_{00}/3)d\sigma/dt$$

project out helicity zero $\bar{K}^*$ production via unnatural parity exchange (σ_0) and, to order (1/s), helicity one $\bar{K}^*$ production via natural (σ_+) and unnatural (σ_-) parity exchange. The decomposition of the $K\pi$ differential cross section into σ_+ and into σ_0 and σ_- in the s-channel is also presented in Fig. 3.

Since the six experimentally measurable moments do not determine the seven s,p wave density matrix elements, each $\bar{K}^*$ partial cross section contains a small $K\pi$ s-wave background. Previous measurements of $K\pi$ scattering phase

shifts in this mass region [7,8] provide an estimate of the s-wave strength relative to the m=0, p-wave. Using an s-wave phase shift of 35°, $\rho_{00}^{00}/\rho_{00}^{11} = 0.14$. Furthermore, an experimental upper limit on the s-wave contribution is provided by the σ_- distribution. The s-wave differential cross section, which should resemble σ_0 in shape, can at most account for the observed σ_- cross section at the dip near $t \sim m_\pi^2$. Thus the factor $\rho_{00}^{00}/3$ only makes a small contribution even for the σ_+ and σ_- distributions.

The dominant exchange contributions for $\bar{K}^*$ production may be inferred directly from the data by comparing our results with those for $\pi^- p \rightarrow \rho^o n$ [3,4]. The helicity zero cross section, σ_0, displays the strong forward t dependence expected for the dominant π exchange amplitude. Its shape is very similar to that observed for ρ production indicating that B exchange contributions which are allowed for $\bar{K}^*$ production are probably small. Both σ_0 and the density matrix element combination $\rho_{00} - \rho_{11}$ exhibit forward turnovers in both the s- and t-channels.

The density matrix elements Re ρ_{10}^{11} and Re ρ_{10}^{10} both exhibit a rapid variation at small momentum transfer in the s-channel with the zero crossover near $|t| \sim 0.011$ GeV^2. This result differs significantly from $\pi^- p \rightarrow \rho^o n$ data [3,4] where the crossover zero occurs at $|t| = m_\pi^2$. The crossover location corresponds to a zero in the unnatrual exchange helicity one amplitude and is associated with π exchange absorptive effects. The shift in the crossover location then implies that an additional term is present in the m = 1 unnatural exchange amplitude for $\bar{K}^*$ production at small t.

The density matrix element ρ_{1-1}^{11} and the natural exchange cross section σ_+ are very much larger for the $\bar{K}^*$ data than for the ρ data in the intermediate t region around 0.2 GeV^2. This is due presumably to a large ρ exchange

contribution to the $\bar{K}^*$ production in addition to the A_2 contribution, which for ρ production is the only natural parity exchange allowed by G parity conservation. From Fig. 3 it is seen that natural parity exchange is the dominant contribution to $\bar{K}^*$ production for $|t| > 0.16$ GeV^2. It is this marked transition from the dominance of π exchange at small t to the much flatter t-dependence of the ρ and A_2 exchange that accounts for the flattening of the $\bar{K}^*$ differential cross section in this t region. σ_+ also exhibits a significant forward dip near $t \approx 0$. However, this dip cannot be simply and directly associated with ρ exchange since there is a large contribution to the σ_+ cross section in the $|t| \approx m_\pi^2$ region from π exchange absorptive effects. Comparison of these data with 4 and 6 GeV $K^-p \rightarrow K^-\pi^+n$ data [2] shows that the energy dependence of σ_+ near $|t| = m_\pi^2$ is the same as that of σ_0, i.e., it is related to π exchange, whereas the relative contribution of σ_+ to the $\bar{K}^*$ cross section for $t > 0.10$ GeV^2 increases substantially with s, as expected for ρ - A_2 exchange.

In conclusion, in this experiment studying $K^-p \rightarrow \bar{K}^*(890)n$ we have observed the pronounced forward t structure of the s-channel density matrix elements previously seen in $\pi^-p \rightarrow \rho^0n$ data. Furthermore, by comparison of the $\bar{K}^*$ results with $\pi^-p \rightarrow \rho^0n$ analyses, we may conclude that π exchange with absorption will qualitatively account for the forward structure observed. In the intermediate and large momentum transfer region, the natural parity ρ-A_2 exchange contribution dominates. A quantitative analysis of the $\bar{K}^*$ amplitude structure will be presented separately.

REFERENCES

[1] For some previous experimental results see:

M. Aguilar-Benitez et al., Phys. Rev. Lett. 26 (1971) 466;

M. Deutschmann et al., Nucl. Phys. B36 (1972) 373;

B. Chaurand et al., Phys. Lett. 38B (1972) 253;

M. Deutschmann et al., Nucl. Phys. B81 (1974) 1.

[2] A. B. Wicklund et al., contributed paper #99, XVII Int. Conf. on High Energy Physics, London, 1-10 Jul 1974.

[3] F. Bulos et al., Phys. Rev. Lett. 26 (1971) 1453;

P. Baillon et al., Phys. Lett. 35B (1971) 453.

[4] G. Grayer et al., Nucl. Phys. B50 (1972) 29;

P. Estabrooks and A. D. Martin, Phys. Lett. 41B (1972) 350;

B. Hyams et al., Phys. Lett. 51B (1974) 272.

[5] G. Brandenburg et al., to be submitted to Nucl. Instr. and Meth.

[6] The missing mass squared resolution is $\sigma(MM^2) = 0.18\ GeV^2$.

[7] H. H. Bingham et al., Nucl. Phys. B41 (1972) 1.

[8] M. J. Matison et al., Phys. Rev. D 9 (1974) 1872.

FIGURE CAPTIONS

1. Plan view of the experimental apparatus.

2. Density matrix elements for $K^-p \rightarrow K^-\pi^+n$ at 13 GeV for $0.87 < m(K^-\pi^+) < 0.92$ GeV in the s-channel helicity frame.

3. Differential cross section for $K^-p \rightarrow K^-\pi^+n$ at 13 GeV for $0.87 < m(K^-\pi^+) < 0.92$ GeV. The partial cross sections σ_0 and σ_- correspond to helicity zero and one $\bar{K}^*$ production by unnatural parity exchange in the s-channel. σ_+ corresponds to helicity one $\bar{K}^*$ production by natural parity exchange. Each contains a small s-wave component. (See text.)

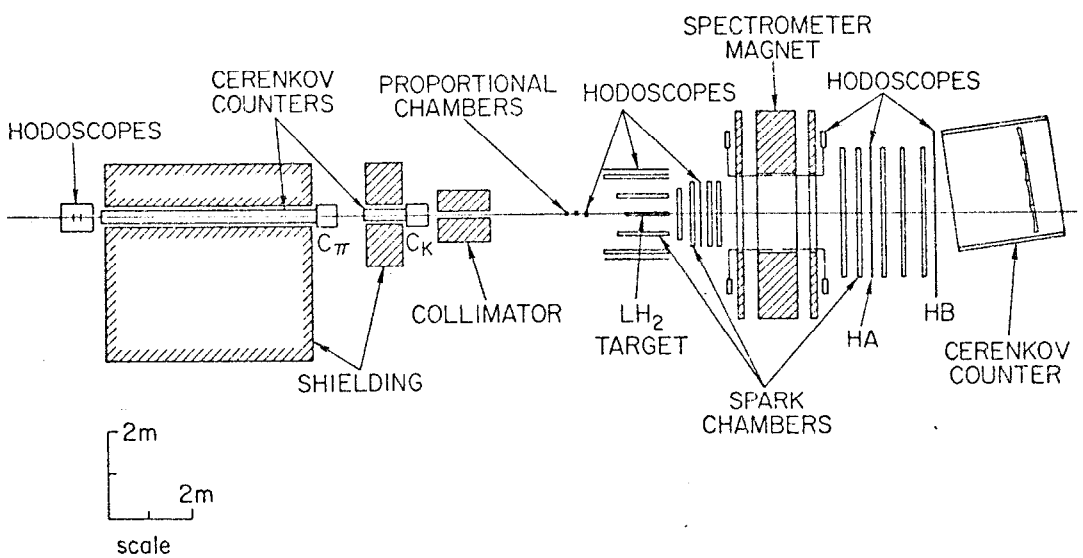

Fig. 1

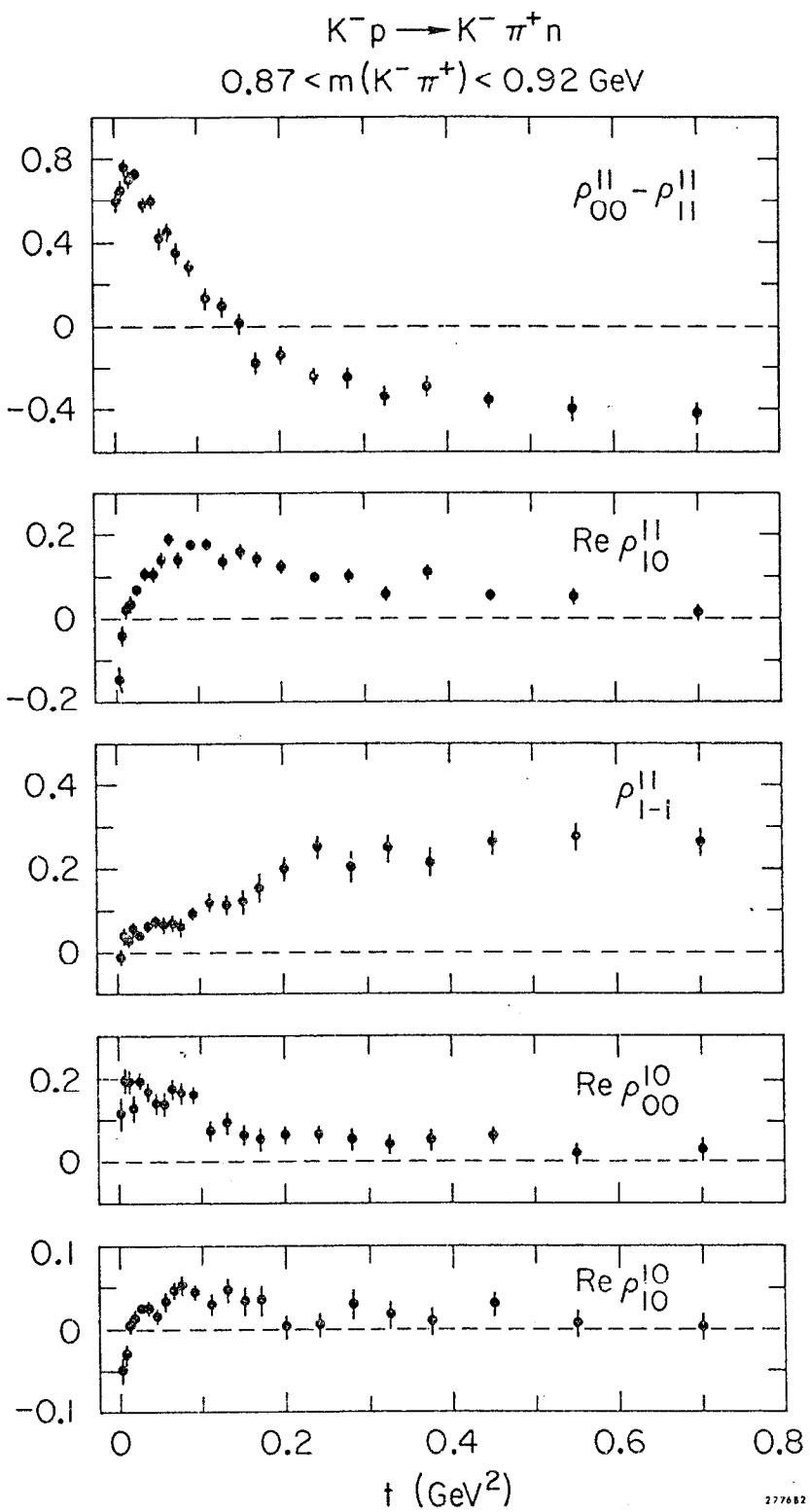
K⁻p → K⁻ π⁺n
0.87 < m(K⁻ π⁺) < 0.92 GeV
$\rho^{11}_{00} - \rho^{11}_{11}$
Re ρ^{11}_{10}
ρ^{11}_{1-1}
Re ρ^{10}_{00}
Re ρ^{10}_{10}
0.8
0.4
0
-0.4
0.2
0
-0.2
0.4
0.2
0
0.2
0
0.1
0
-0.1
0
0.2
0.4
0.6
0.8
t (GeV²)
277682

Fig. 2

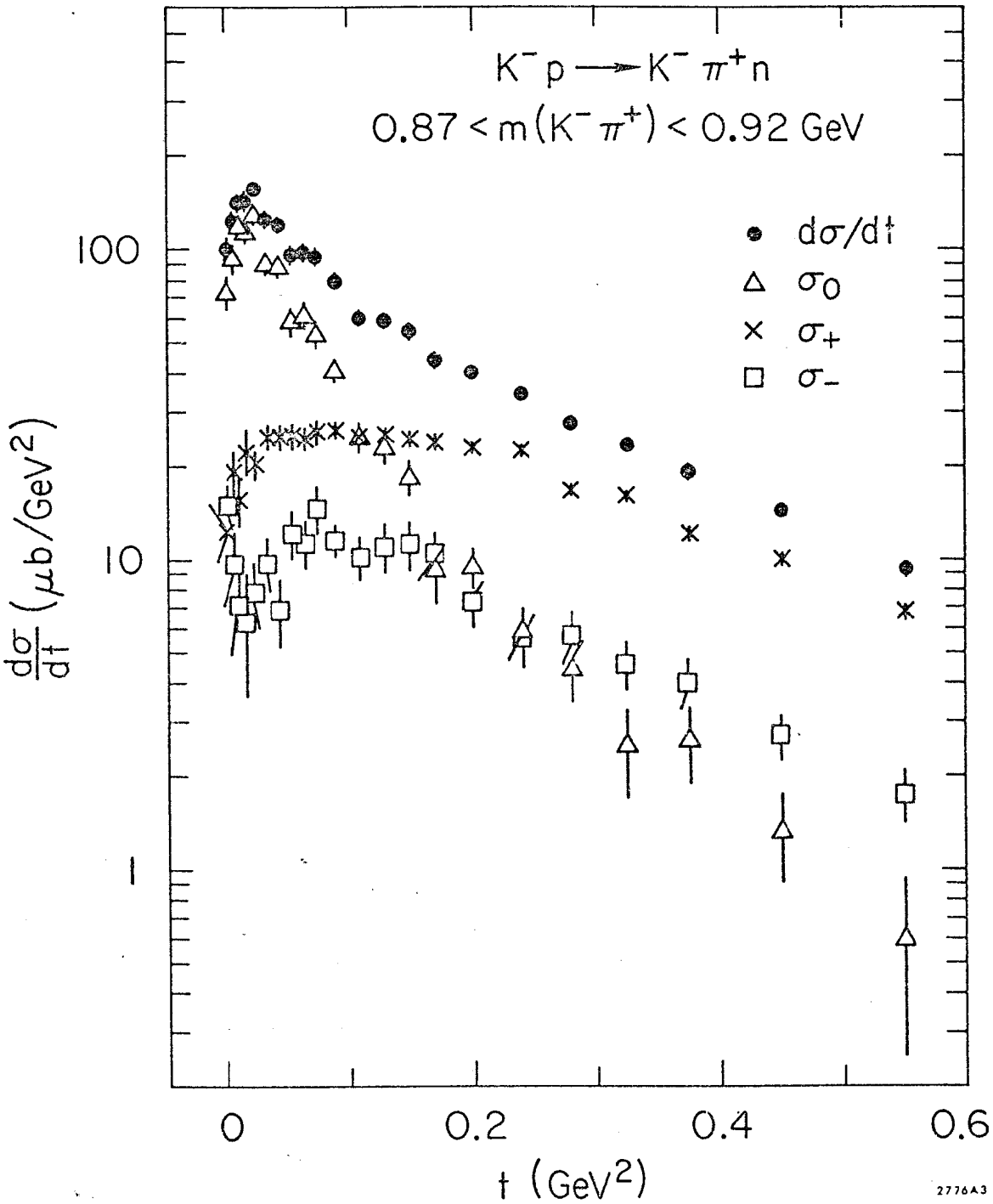
K⁻p → K⁻π⁺n
0.87 < m(K⁻π⁺) < 0.92 GeV
dσ/dt
σ0
σ+
σ−
100
10
1
dσ/dt (μb/GeV²)
0
0.2
0.4
0.6
t (GeV²)
2776A3

Fig. 3